

Discovering intermediate-mass black hole lenses through gravitational wave lensing

Kwun-Hang Lai,^{1,*} Otto A. Hannuksela,^{1,†} Antonio Herrera-Martín,² Jose M. Diego,³ Tom Broadhurst,^{4,5} and Tjonnie G. F. Li¹

¹*Department of Physics, The Chinese University of Hong Kong, Shatin, NT, Hong Kong*

²*SUPA, University of Glasgow, Glasgow, G12 8QQ, United Kingdom*

³*Instituto de Física de Cantabria (IFCA, UC-CSIC), Av. de Los Castros s/n, E-39005 Santander, Spain*

⁴*Department of Theoretical Physics, University of Basque Country UPV/EHU, Bilbao, Spain*

⁵*IKERBASQUE, Basque Foundation for Science, Bilbao, Spain*

(Dated: November 27, 2018)

Intermediate-mass black holes are the missing link that connects stellar-mass to supermassive black holes and are key to understanding galaxy evolution. Gravitational waves, like photons, can be lensed, leading to discernable effects such as diffraction or repeated signals. We investigate the detectability of intermediate-mass black hole deflectors in the LIGO-Virgo detector network. In particular, we simulate gravitational waves with variable source distributions lensed by an astrophysical population of intermediate-mass black holes, and use standard LIGO tools to infer the properties of these lenses. We find detections of intermediate-mass black holes at 98% confidence level over a wide range of binary and lens parameters. Therefore, we conclude that intermediate-mass black holes could be detected through lensing of gravitational waves in the LIGO-Virgo detector network.

INTRODUCTION

The existence of stellar-mass and supermassive black holes (SMBHs) has become widely accepted due to X-ray observations of X-ray binary systems [1, 2] and measurements of the orbits of stars in the center of the Milky Way [3–5]. While the existence of SMBHs is widely accepted, their formation is a mystery due to a black hole (BH) mass gap in the range ($\sim 10^2 - 10^5 M_\odot$). Black holes in this mass range are called intermediate-mass black holes (IMBHs). We have yet to observe these BHs but expect to see a transition from stellar-mass to supermassive BHs [6, 7]. Finding this link is crucial to understanding the formation of SMBHs and galaxies.

Only indirect evidence for IMBHs exists [8], but there are multiple active detection efforts. A recent study focusing on mapping the potential of the globular cluster 47 Tucanae through pulsar timing in combination with N-body simulations casts indirect evidence towards an IMBH in the center of the cluster [9]. However, the potential for this cluster was derived from N-body simulations subject to a degree of model uncertainty [see 10, for a review of the method]. Other forms of searches involve locating X-ray and radio emissions from accretion onto IMBHs, finding tidal disruption events, looking for IMBH imprints in molecular clouds and microlensing experiments [11]; for a review, see [8]. Despite the many efforts to detect IMBHs, the evidence is still inconclusive.

Gravitational lensing is the bending of light, waves or particles near concentrated mass distributions. Lensing events probe the IMBH's potential, opening a promising avenue for detection. On 14 September 2015, the first gravitational wave event was observed with Laser Interferometer Gravitational-Wave Observatory (LIGO) [12]. Similarly to light, gravitational waves (GWs) can be influenced by gravitational lensing [13–19]. When the wavelength of GWs is comparable to

the Schwarzschild radius of the lens, diffraction effects become relevant to the treatment of the lens effect [18]. In the LIGO band, these wave effects happen in the IMBH mass range.

There is a growing body of research suggesting that LIGO will see several lensed gravitational-wave events [20, 21]. Einstein Telescope (ET), a future ground-based GW detector will see a thousand-fold more. However, previous research has focused on galaxy lensing, while we focus on IMBH lenses. We have calculated the approximate number of GW events lensed by IMBHs in LIGO (ET), arriving at ~ 0.05 (~ 50) events/year. For the full calculation, see the "rates" section.

Cao et al. 2014 [22] investigated the effect of lensing on GW parameter estimation using Markov-Chain Monte Carlo to study the lens degeneracy between lens parameters in the LIGO framework. In this work, we show that IMBHs may be detected through lensed events in a realistic LIGO-Virgo detector network. We use realistic gravitational-wave inspiral merger ringdown waveform [23] which is utilized in real LIGO searches. By inclusion of spin in our waveform model we account for the possibility that spin precession of the binary [see 24] could mimic lensing. In addition, we consider an Advanced LIGO and Virgo detection network at design sensitivity [25, 26]. Moreover, we study the parameter constraints in realistic lensing scenarios by including a wide range of lens masses.

Our results show that lensed GWs can be used to infer the mass of IMBHs, providing a novel avenue to detect them. In particular, if a GW is lensed through a potential induced by an IMBH in our parameter range, we can claim detection with 98% confidence in $\sim 20\%$ of the cases. Moreover, we show that we can distinguish astrophysical larger than $\sim 8 \times 10^3$ AU from IMBHs (typical Schwarzschild radius $\sim 10^{-5}$ AU). Structures smaller than this act effectively as point lenses. Finally, we discuss the implications of our results on detection of IMBHs.

* adrian.k.h.lai@link.cuhk.edu.hk

† hannuksela@phy.cuhk.edu.hk

METHODS

Consider a system composed of a source emitting GWs, a lens, and a distant observer. The source must be close (sub-parsec scale) to the line-of-sight between the lens and the observer for lensing to occur; we denote this distance with η . The angular diameter distances along the line-of-sight between source-lens, source-observer, and lens-observer, are denoted as D_{LS} , D_S , and D_L , respectively. IMBHs can be approximated as point mass lenses [19]. Given that we ignore the near horizon contribution to the lensing effect, the lensed waveform $h_{+, \times}^{\text{lensed}}(f)$ is [18, 19]

$$h_{+, \times}^{\text{lensed}}(f) = F(w, y)h_{+, \times}^{\text{unlensed}}(f), \quad (1)$$

where

$$F(w, y) = \exp \left[\frac{\pi w}{4} + i \frac{w}{2} \left\{ \ln \left(\frac{w}{2} \right) - \frac{(\sqrt{y^2 + 4} - y)^2}{4} \right. \right. \\ \left. \left. + \ln \left(\frac{y + \sqrt{y^2 + 4}}{2} \right) \right\} \right] \Gamma \left(1 - \frac{i}{2} w \right) \\ \times {}_1F_1 \left(\frac{i}{2} w, 1; \frac{i}{2} w y^2 \right), \quad (2)$$

where $h_{+, \times}^{\text{unlensed}}$ is the waveform without lensing, Γ is complex gamma function, ${}_1F_1$ is confluent hypergeometric function of the first kind, $w = 8\pi M_{Lz} f$ is dimensionless frequency, $M_{Lz} = M_L(1 + z_L)$ is the redshifted lens mass, $y = D_L \eta / \xi_0 D_S$ is the source position, $\xi_0 = (4M_L D_L D_{LS} / D_S)^{1/2}$ is a normalization constant (Einstein radius for point mass lens), and M_L and z_L are the lens mass and redshift, respectively. The magnification function includes the information of the time delay and is not to be confused with its geometric optics counterpart. To calculate the magnification function $F(w, y)$, we construct a lookup table, and retrieve its values by bilinear interpolation; the error between the table and the exact solution is less than 0.1%. For the GW waveform, we use IMRPhenomPv2 model, which includes the whole binary inspiral-merger-ringdown phase [27]. This assumes an isolated point lens, but we also discuss the effect of external shear and host galaxy in the last section.

We inject GW signals from an astrophysical population of binary sources lensed by IMBHs into mock noise data and infer the properties of the IMBH lens. The motivation for choosing a distribution of simulated signals is to ensure that we can detect lensed signals across variable lens and binary properties. This is in contrast to focusing on a single "example" scenario, which can be fine-tuned. Following [28], the astrophysical distribution of the binary source is uniform in component masses, dimensionless spin magnitude, and volume; isotropic in spin directions and in sky location. We assume isolated lenses distributed uniformly in volume, i.e. $P(y) \propto y^2$ [19], where we cut the distribution off at $y > 3$ when lensing effects become small ($F \sim 1$) and at $y < 0.1$ which makes

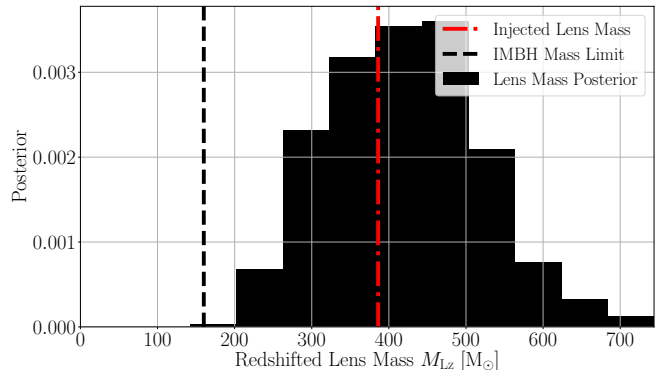


FIG. 1. An example redshifted lens mass posterior distribution recovered from an injected, lensed gravitational wave signal using nested sampling (LALInference). The red dashed line shows the injected redshifted lens mass ($\sim 390M_{\odot}$) and the black dashed line shows the intermediate-mass black hole (IMBH) mass lower bound ($160M_{\odot}$). All of the posterior samples are above the lower bound of IMBH mass.

up only a fraction of the lensed events. We distribute redshifted lens mass uniformly in $M_{Lz} \in [1, 1000]M_{\odot}$, which includes the lower IMBH mass range and extends to stellar-mass range. Taking larger masses implies more pronounced lensing effects, and therefore our mass range tests the weak lensing limit. If the lens is not isolated, i.e., more lenses are concentrated in the vicinity of galaxies, then the distribution requires corrections. These corrections would likely favour nearer sources because most galaxies are at $z \sim 0.3$ [29]. However, the study of such realistic source distributions requires numerical simulations and is outside the scope of this work. Finally, we limit the unlensed signal-to-noise (SNR) distribution to be $\rho \in [8, 32]$, because LIGO requires an SNR of at least 8 for claiming a detection, and signals with SNR greater than 32 are rare [30]. We take four different source mass scenarios to investigate the effect of mass ratio on parameter inference.

We infer the lens mass using nested sampling algorithm (LALInference) [31]. The lens mass and lens redshift are fully degenerate with each other. However, in the range detectable by LIGO [32], the Hubble Deep Field survey shows that the majority of the galaxies that can harbor IMBHs are located at $z_L \sim 0.6$ [29], which can be used as an approximate, typical redshift in our analysis. Therefore, we choose the probability $P(M_{Lz} > 160M_{\odot}) > 98\%$ to indicate a successful detection of IMBH. We show an example redshifted lens mass posterior distribution recovered from an injected GW that passes through a lens of mass $M_L \approx 380M_{\odot}$ (Fig. 1). The posterior peaks around the injected value and the samples are above the IMBH mass limit. In our analysis, this posterior is classified as detection.

LENSING EVENT RATES

The number of GW events lensed by IMBHs may be estimated using the known GW event rates and assuming an IMBHs lens population. Astrophysical modeling suggests that around 20% of globular clusters could harbor IMBHs [35]. In that case, by order of magnitude, we have $\sim 10^2 - 10^4$ IMBHs per galaxy [33, 34], which is in agreement with N-body simulations of molecular clouds reach similar number of IMBHs in galaxies [36]. We assume a typical $n \sim 0.03 \text{ Mpc}^{-3}$ density of galaxy lenses at $z_L \sim 0.3 - 0.6$ [37, 38], angular diameter distance to lens $D_L \sim 800 \text{ Mpc}$, and from lens to source $D_{LS} \sim 800 \text{ Mpc}$. The probability of a single event being lensed is given by the area of the lens in the lens plane, which to the first order can be computed as the area within the Einstein radius, divided by the total area of the lens plane. The Einstein radius of the IMBH lens within a galaxy is boosted by a typical galaxy magnification $\mu \sim 2 - 3$, which also boost the probability of it being lensed. The rate of unlensed events is $\sim 800 - 10000$ events/year at design sensitivity of Advanced LIGO [21, 39] (and 1000 times more at ET sensitivity), based on rates inferred directly by LIGO. Therefore, the total number of lensed events boosted by magnification μ is $R_{\text{lensed}} \sim 10^{-14} (M_L/M_\odot) N_{\text{IMBH}} N_{\text{GW}} \mu^{5/2} \sim 3.74 \times 10^{-6} - 0.16$ events/year at design sensitivity ($\sim 3.74 \times 10^{-3} - 160$ events/year in ET), where the lower and upper bound are given by pessimistic and optimistic parameters respectively. However, taking typical IMBH candidate mass [35, 40] and lens populations [41] as an example yields $R_{\text{lensed}} \sim 10^{-14} (M_L/M_\odot) N_{\text{IMBH}} N_{\text{GW}} \mu^{5/2} \sim 10^{-14} \times (5000 M_\odot/M_\odot) \times 10^4 \times 6000 \times 3^{5/2} \sim 0.05$ events/year (50 events/year in ET). This is roughly comparable to the microlensing event rates for IMBHs in the electromagnetic band, which stand at 0.86 events/(20 years) [42]. The $5000 M_\odot$ is a more massive lens than what we consider as a reference in our nested sampling study, but our results are applicable in this mass regime as well because it is easier to detect larger lens masses tend due to larger lens effects. Such a number assumes that IMBH candidates are within the range of thousands of solar masses [35, 40] and the number of IMBHs is around 10^4 per galaxy [41].

We stress that having precise event rate estimates is difficult due to the large uncertainty in the number density of IMBHs, the event rates of binary coalescences, uncertainty in IMBH mass distribution and the uncertainty in the lens magnification distribution. Therefore, the event rate should be taken as an order-of-magnitude estimate demonstrating that detecting lensing by IMBHs is possible. Nevertheless, if we do detect a GW signal lensed by an IMBH, we have a chance to discriminate it using the methods we outline in this work.

DETECTING INTERMEDIATE-MASS BLACK HOLES

We find detections over a wide range of lens masses ($M_{Lz} \gtrsim 200 M_\odot$), and find a rising trend in detections with higher

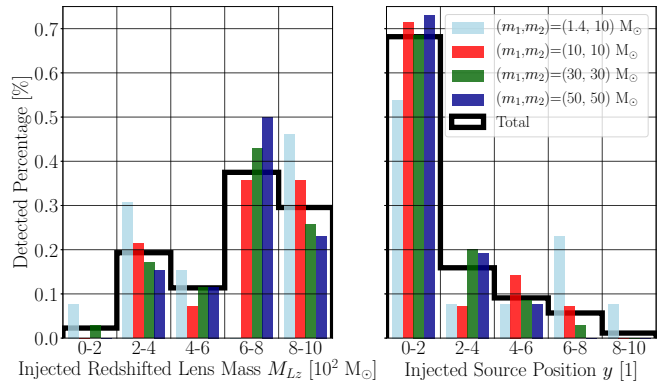


FIG. 2. Detected intermediate-mass BHs as a function of injected redshifted lens mass M_{Lz} (left panel), and source position squared y^2 (right panel) for four different source binary masses and their sum. Detection is defined at 98% confidence level. The number of detections decreases with increasing source positions, and increases with increasing lens masses.

lens mass (Fig. 2, left panel). Of these, we find around $\sim 16 - 30\%$ of detected IMBHs with relatively small redshifted lens masses ($M_{Lz} < 500$; Fig. 2). Approximately 20% of lenses are detectable in our parameter range. However, there are two false alarms with masses lower than $160 M_\odot$, which is statistically expected at 98% confidence level, given that we have over 100 detections.

In addition to redshifted lens mass, we characterize the effect of source position on the detectability of IMBHs. The source position y is proportional to the horizontal distance from the line-of-sight. Because smaller source positions y correspond to larger lens effects, we expect better constraints at small y . Indeed, we detect a more substantial number of IMBHs at low source positions, where more than 55% of them are in the range $y^2 = [0, 2.5]$ for all source masses (Fig. 2, right panel). Meanwhile, we find that there are also detections at relatively large source positions ($y^2 > 5$) but the number decreases for increasing position. The source position at $y = \sqrt{2.5} \approx 1.58$ can be translated back to the displacement from the line-of-sight. Assuming typical lens-to-source distance $D_{LS} = 300 \text{ Mpc}$, lens distance $D_L = 300 \text{ Mpc}$ and source distance $D_S = 600 \text{ Mpc}$, we have $\eta \approx 0.01 \text{ pc} \sqrt{M_L/M_\odot}$. Hence, the line-of-sight distance where we detect IMBHs is likely sub-parsec.

We detect IMBHs across the SNR range $\rho \in [9, 32]$. To put this into the context of the current LIGO detections, all of the confirmed detections have had a network inferred SNR inside our range (see the first observing run summary [43]).

In all four classes of source mass realizations, we detect around 20% of the IMBHs at a 98% confidence level. Among the detected signals, we also compare the Bayes factors between the lensed model and the unlensed model. The evidence for the lensed hypothesis is significantly (400 times) larger than the unlensed hypothesis for more than 70% of the signals, which suggests that these detections are not cause by

noise. Moreover, we have simulated and analyzed a set of unlensed signals. Of these, none prefer the lensed hypothesis at Bayes factor above 40. The lensing effect is not degenerate with sky location and other parameters, and therefore calibration uncertainties are not expected to affect the results drastically [see e.g. 44, 45, for review]. Therefore, we are confident that the detection criteria $P(M_{Lz} > 160M_{\odot}) > 98\%$ together with the Bayes factor analysis provide a reasonable estimate of the detectability of IMBH. We have also analyzed the first GW event GW150914 [12], finding no evidence of lensing (Bayes factors both being the same up to 4th significant digit for the lensed and unlensed case).

In conclusion, we find detections across $M_{Lz} \in [160, 1000]M_{\odot}$, $y^2 \in [0.01, 9]$ and $\rho \in [9, 32]$, and find that higher lens masses, smaller source positions and higher SNR are favored.

DISCRIMINATING BETWEEN POINT AND FINITE-SIZE LENS

Other small astrophysical lens objects could mimic IMBH lenses. We study a finite-size singular isothermal sphere (SIS) model to test our ability to discriminate between finite and point lenses using GWs. If the size is small enough, the object will collapse into a BH. The SIS model represents the approximate mass distribution of an extended astrophysical object. Its magnification function [19]

$$F_{\text{SIS}}(w, y) = -iw e^{iwy^2/2} \int_0^{\infty} dx \left\{ x J_0(wxy) \times \exp \left[iw \left(\frac{1}{2}x^2 - x + y + \frac{1}{2} \right) \right] \right\}, \quad (3)$$

where $w = 8\pi M_{Lz} f$, $M_{Lz} = 4\pi^2 v^4 (1 + z_L) D_L D_{LS} / D_S$ is the redshifted mass inside the Einstein radius ξ_0 , v is a characteristic dispersion velocity of the model and $x = |\vec{\xi}/\xi|$ is the normalized impact parameter. We expect the SIS model to be indistinguishable from an IMBH model due to mass screening effect when the Einstein radius ξ_0 is small.

In order to compare the SIS and the point lens model, we compute the match $m(h_a, h_b)$ [46, 47] between two waveforms h_a and h_b maximized over time, phase and amplitude. For this comparison, we simulate GWs from a (30,30) M_{\odot} source oriented in the overhead direction and compare the match between the signals lensed by an SIS and a point lens.

We consider different pairs of (M_{Lz}, y) , and maximize the $m(h_a, h_b)$ by non-linear least squares fitting and classify $m(h_a, h_b) < 97\%$ as distinguishable in LIGO waveform following [48]. We show that the SIS lens and point lens can be discriminated when redshifted lens mass $M_{Lz} > 200M_{\odot}$, shown as a match lower than 97% in Fig. 3. The source positions $y = 1$ and $y = 0.1$ show higher match for all redshifted lens masses because small source positions y cause only a total magnification of the signal, while very large y cause only small lens effect. The oscillatory property of the magnifica-

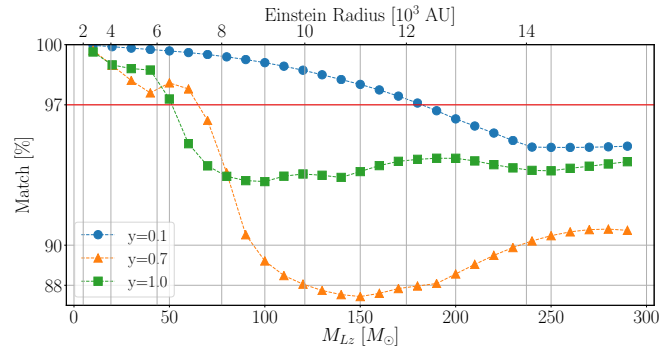


FIG. 3. Match $m(h_a, h_b)$ between waveform lensed by an SIS and a point mass lens maximized by non-linear least-squares fitting as a function of redshifted lens mass M_{Lz} (bottom axis) and Einstein radius (top axis). Three source positions $y = 0.1$, $y = 0.7$ and $y = 1.0$ are shown as dashed lines with blue circles, orange triangles, and green squares, respectively. The red horizontal line denotes 97% match. The source and source-to-lens angular diameter distances are chosen so that the lens is in the middle with $D_L = D_{LS} = 400\text{Mpc}$. At redshifted lens mass $M_{Lz} = 200M_{\odot}$ all matches are below 97%.

tion functions F and F_{SIS} induces the oscillatory dependency between the match and M_{Lz} .

The SIS model has an intrinsic length scale, which is the Einstein radius. Since astrophysical structures with diameters smaller than 10^4AU show high match (Fig. 3), they can not be discriminated from point lenses. Indeed, our results suggest we can distinguish an IMBH from a globular cluster (half-mass radius at pc scale [49]), but not structures smaller than 10^4AU .

DISCUSSION AND CONCLUSIONS

We demonstrate that it is possible to discover IMBHs in the LIGO-Virgo network by analyzing GWs lensed by these BHs even for relatively small lens masses ($M_L \sim 200 - 300M_{\odot}$). We find that in $\sim 20\%$ of cases the effect of lensing is strong enough to discover an IMBH with 98% confidence in our parameter range. Moreover, we find that we can discriminate between SIS and point lens models when the Einstein radius of the SIS is larger than 10^4AU . In particular, our results suggest that we may discriminate an IMBH lens from an extended astrophysical object, but it is hard to distinguish between IMBH lenses and compact objects of similar mass. However, there is currently no conclusive evidence of compact objects with masses greater than $200M_{\odot}$.

In our results, we do not account for shear effects by host galaxies. However, it is important to discuss its effect on the results, as compact objects are typically discovered as part of a galaxy. Such shear magnifies the GW signal and introduces a degeneracy between the inferred lens mass and shear magnification. In particular, external shear enlarges the point lens' Einstein radius, stretching it along the deflection field of the host galaxy and changing the lens time delay [see

50]. Consequently, the effective mass of the lens becomes $M'_L \rightarrow \mu_t \times M_L$ owing to its dependence on the Einstein radius. The stretching is modest when the magnification by galaxy μ_{gal} is reasonably low ($\mu_{\text{gal}} \lesssim 5$), and the new radius is larger by a factor of $\sim \mu_t^{1/2}$, with μ_t being the tangential magnification component. The lensing probability at high magnification goes as μ_{gal}^{-2} . As a consequence, typical magnifications are modest, between $\mu_{\text{gal}} \sim 1 - 3$. Taking such typical shear and magnification, we would need to measure 300 M_\odot lens to distinguish the lens as an IMBH. Meanwhile, the magnification in shear would boost the GW event rates.

In contrast with previous results, our results imply that we can detect IMBHs within LIGO data. However, there is also an interesting prospect of detecting stellar mass BHs with GWs. LIGO may not be sensitive enough to constrain the properties of $\sim 1M_\odot$ lenses and the event rate required for GWs lensed by $\sim 30M_\odot$ lenses with high enough SNR may be too low, but there is an interesting prospect of detecting these BHs with future third-generation detectors such as the Telescope and Cosmic Explorer [see 51–54]; these prospects are discussed by [55].

Moreover, IMBH could be directly detected by LIGO; however, these detections are limited to a mass range $M \lesssim 150M_\odot$ due to the low-frequency noise in LIGO [36]. Our method does not suffer from such cut-off, and its discriminatory power increases for more massive lenses.

In conclusion, we have shown that lensing of GWs by IMBHs is detectable over a wide range of parameters and that a detection of a point mass lens of mass higher than $300M_\odot$ in principle warrants a discovery of IMBHs. In the future, we will expand our study on the effect of different lensing models, and mixed models with BHs and surrounding matter; for example, it is essential to investigate lens models with globular clusters containing IMBHs and lenses admixed in shear.

-
- [1] Jeffrey E McClintock and Ronald A Remillard. Black hole binaries. *arXiv preprint astro-ph/0306213*, 2003.
- [2] Ronald A Remillard and Jeffrey E McClintock. X-ray properties of black-hole binaries. *Annu. Rev. Astron. Astrophys.*, 44:49–92, 2006.
- [3] AM Ghez, S Salim, SD Hornstein, A Tanner, JR Lu, M Morris, EE Becklin, and G Duchêne. Stellar orbits around the galactic center black hole. *The Astrophysical Journal*, 620(2):744, 2005.
- [4] AM Ghez, S Salim, NN Weinberg, JR Lu, T Do, JK Dunn, K Matthews, MR Morris, S Yelda, EE Becklin, et al. Measuring distance and properties of the milky ways central supermassive black hole with stellar orbits. *The Astrophysical Journal*, 689(2):1044, 2008.
- [5] John Kormendy and Luis C Ho. Coevolution (or not) of supermassive black holes and host galaxies. *Annu. Rev. Astron. Astrophys.*, 51:511–653, 2013.
- [6] Steinn Sigurdsson and Lars Hernquist. Primordial black holes in globular clusters. *Nature*, 364(6436):423–425, 1993.
- [7] Toshikazu Ebisuzaki, Junichiro Makino, Takeshi Go Tsuru, Yoko Funato, Simon Portegies Zwart, Piet Hut, Steve McMillan, Satoki Matsushita, Hironori Matsumoto, and Ryohei Kawabe. Missing link found? the runaway path to supermassive black holes. *The Astrophysical Journal Letters*, 562(1):L19, 2001.
- [8] Mar Mezcua. Observational evidence for intermediate-mass black holes. *International Journal of Modern Physics D*, page 1730021, 2017.
- [9] Bülent Kızıltan, Holger Baumgardt, and Abraham Loeb. An intermediate-mass black hole in the centre of the globular cluster 47 tucanae. *Nature*, 542(7640):203–205, 2017.
- [10] Holger Baumgardt. N-body modelling of globular clusters: masses, mass-to-light ratios and intermediate-mass black holes. *Monthly Notices of the Royal Astronomical Society*, 464(2):2174–2202, 2016.
- [11] Roeland P Van Der Marel. Intermediate-mass black holes in the universe: a review of formation theories and observational constraints. *Coevolution of Black Holes and Galaxies*, page 37, 2004.
- [12] Benjamin P Abbott, Richard Abbott, TD Abbott, MR Abernathy, Fausto Acernese, Kendall Ackley, Carl Adams, Thomas Adams, Paolo Addesso, RX Adhikari, et al. Observation of gravitational waves from a binary black hole merger. *Physical review letters*, 116(6):061102, 2016.
- [13] Hans C Ohanian. On the focusing of gravitational radiation. *International Journal of Theoretical Physics*, 9(6):425–437, 1974.
- [14] PV Bliokh and AA Minakov. Diffraction of light and lens effect of the stellar gravitation field. *Astrophysics and Space Science*, 34(2):L7–L9, 1975.
- [15] Robert J Bontz and Mark P Haugan. A diffraction limit on the gravitational lens effect. *Astrophysics and Space Science*, 78(1):199–210, 1981.
- [16] Kip S Thorne. The theory of gravitational radiation—an introductory review. In *Gravitational radiation*, pages 1–57, 1983.
- [17] Sh Deguchi and WD Watson. Diffraction in gravitational lensing for compact objects of low mass. *The Astrophysical Journal*, 307:30–37, 1986.
- [18] Takahiro T Nakamura. Gravitational lensing of gravitational waves from inspiraling binaries by a point mass lens. *Physical review letters*, 80(6):1138, 1998.
- [19] Ryuichi Takahashi and Takashi Nakamura. Gravitational lensing of gravitational waves. *The Astrophysical Journal*, 595:1039–1051, 2003.
- [20] Liang Dai, Tejaswi Venumadhav, and Kris Sigurdson. Effect of lensing magnification on the apparent distribution of black hole mergers. *Physical Review D*, 95(4):044011, 2017.
- [21] Ken KY Ng, Kaze WK Wong, Tom Broadhurst, and Tjonnie GF Li. Precise ligo lensing rate predictions for binary black holes. *Physical Review D*, 97(2):023012, 2018.
- [22] Zhoujian Cao, Li-Fang Li, and Yan Wang. Gravitational lensing effects on parameter estimation in gravitational wave detection with advanced detectors. *Physical Review D*, 90(6):062003, 2014.
- [23] Mark Hannam, Patricia Schmidt, Alejandro Bohé, Leïla Haegel, Sascha Husa, Frank Ohme, Geraint Pratten, and Michael Pürrer. Simple model of complete precessing black-hole-binary gravitational waveforms. *Physical review letters*, 113(15):151101, 2014.
- [24] Luc Blanchet. Gravitational radiation from post-newtonian sources and inspiralling compact binaries. *Living Reviews in Relativity*, 17(1):2, 2014.
- [25] J. Aasi et al. Advanced LIGO. *Class. Quant. Grav.*, 32:074001, 2015.
- [26] F. Acernese et al. Advanced Virgo: a second-generation in-

- terferometric gravitational wave detector. *Class. Quant. Grav.*, 32(2):024001, 2015.
- [27] Rory Smith, Scott E Field, Kent Blackburn, Carl-Johan Haster, Michael Pürrer, Vivien Raymond, and Patricia Schmidt. Fast and accurate inference on gravitational waves from precessing compact binaries. *Physical Review D*, 94(4):044031, 2016.
- [28] Salvatore Vitale, Davide Gerosa, Carl-Johan Haster, Katerina Chatziioannou, and Aaron Zimmerman. Impact of bayesian prior on the characterization of binary black hole coalescences. *arXiv preprint arXiv:1707.04637*, 2017.
- [29] Stephen DJ Gwyn and FDA Hartwick. The redshift distribution and luminosity functions of galaxies in the hubble deep field. *The Astrophysical Journal Letters*, 468(2):L77, 1996.
- [30] Hsin-Yu Chen and Daniel E Holz. The loudest gravitational wave events. *arXiv preprint arXiv:1409.0522*, 2014.
- [31] John Skilling. Nested sampling. In *AIP Conference Proceedings*, volume 735, pages 395–405. AIP, 2004.
- [32] Salvatore Vitale and Matthew Evans. Parameter estimation for binary black holes with networks of third-generation gravitational-wave detectors. *Physical Review D*, 95(6):064052, 2017.
- [33] S Michael Fall and Qing Zhang. Dynamical evolution of the mass function of globular star clusters. *The Astrophysical Journal*, 561(2):751, 2001.
- [34] JM Diederik Kruijssen and Simon F Portegies Zwart. On the interpretation of the globular cluster luminosity function. *The Astrophysical Journal Letters*, 698(2):L158, 2009.
- [35] M Coleman Miller and Douglas P Hamilton. Production of intermediate-mass black holes in globular clusters. *Monthly Notices of the Royal Astronomical Society*, 330(1):232–240, 2002.
- [36] Hisa-aki Shinkai, Nobuyuki Kanda, and Toshikazu Ebisuzaki. Gravitational waves from merging intermediate-mass black holes. ii. event rates at ground-based detectors. *The Astrophysical Journal*, 835(2):276, 2017.
- [37] Shaun Cole, Peder Norberg, Carlton M Baugh, Carlos S Frenk, Joss Bland-Hawthorn, Terry Bridges, Russell Cannon, Matthew Colless, Chris Collins, Warrick Couch, et al. The 2df galaxy redshift survey: near-infrared galaxy luminosity functions. *Monthly Notices of the Royal Astronomical Society*, 326(1):255–273, 2001.
- [38] Eric F Bell, Daniel H McIntosh, Neal Katz, and Martin D Weinberg. The optical and near-infrared properties of galaxies. i. luminosity and stellar mass functions. *The Astrophysical Journal Supplement Series*, 149(2):289, 2003.
- [39] Benjamin P Abbott, R Abbott, TD Abbott, MR Abernathy, F Acernese, K Ackley, C Adams, T Adams, P Addesso, RX Adhikari, et al. Gw170104: Observation of a 50-solar-mass binary black hole coalescence at redshift 0.2. *Physical Review Letters*, 118(22):221101, 2017.
- [40] Yu-Qing Lou and Yihong Wu. Intermediate-mass black holes in globular clusters. *Monthly Notices of the Royal Astronomical Society: Letters*, 422(1):L28–L32, 2012.
- [41] Daniel P Caputo, Nathan de Vries, Alessandro Patruno, and Simon Portegies Zwart. On estimating the total number of intermediate mass black holes. *Monthly Notices of the Royal Astronomical Society*, 468(4):4000–4005, 2017.
- [42] N Kains, DM Bramich, KC Sahu, and A Calamida. Searching for intermediate-mass black holes in globular clusters with gravitational microlensing. *Monthly Notices of the Royal Astronomical Society*, 460(2):2025–2035, 2016.
- [43] BP Abbott, R Abbott, TD Abbott, MR Abernathy, F Acernese, K Ackley, C Adams, T Adams, P Addesso, RX Adhikari, et al. Binary black hole mergers in the first advanced ligo observing run. *Physical Review X*, 6(4):041015, 2016.
- [44] Salvatore Vitale, Walter Del Pozzo, Tjonnie GF Li, Chris Van Den Broeck, Ilya Mandel, Ben Aylott, and John Veitch. Effect of calibration errors on bayesian parameter estimation for gravitational wave signals from inspiral binary systems in the advanced detectors era. *Physical Review D*, 85(6):064034, 2012.
- [45] Craig Cahillane, Joe Betzwieser, Duncan A Brown, Evan Goetz, Evan D Hall, Kiwamu Izumi, Shivaraj Kandhasamy, Sudarshan Karki, Jeff S Kissel, Greg Mendell, et al. Calibration uncertainty for advanced ligos first and second observing runs. *Physical Review D*, 96(10):102001, 2017.
- [46] Tito Dal Canton et al. Implementing a search for aligned-spin neutron star-black hole systems with advanced ground based gravitational wave detectors. *Phys. Rev.*, D90(8):082004, 2014.
- [47] Samantha A. Usman et al. The PyCBC search for gravitational waves from compact binary coalescence. *Class. Quant. Grav.*, 33(21):215004, 2016.
- [48] Ian Hinder, Lawrence E Kidder, and Harald P Pfeiffer. An eccentric binary black hole inspiral-merger-ringdown gravitational waveform model from numerical relativity and post-newtonian theory. *arXiv preprint arXiv:1709.02007*, 2017.
- [49] Sidney Van den Bergh. A comparison between the half-light radii, luminosities, and ubv colors of globular clusters in m31 and the galaxy. *The Astronomical Journal*, 140(4):1043, 2010.
- [50] Jose M Diego, Nick Kaiser, Tom Broadhurst, Patrick L Kelly, Steve Rodney, Takahiro Morishita, Masamune Oguri, Timothy W Ross, Adi Zitrin, Mathilde Jauzac, et al. Dark matter under the microscope: Constraining compact dark matter with caustic crossing events. *arXiv preprint arXiv:1706.10281*, 2017.
- [51] M Punturo, M Abernathy, F Acernese, B Allen, Nils Andersson, K Arun, F Barone, B Barr, M Barsuglia, M Beker, et al. The einstein telescope: a third-generation gravitational wave observatory. *Classical and Quantum Gravity*, 27(19):194002, 2010.
- [52] Benjamin P Abbott, R Abbott, TD Abbott, MR Abernathy, K Ackley, C Adams, P Addesso, RX Adhikari, VB Adya, C Affeldt, et al. Exploring the sensitivity of next generation gravitational wave detectors. *Classical and Quantum Gravity*, 34(4):044001, 2017.
- [53] Sheila Dwyer, Daniel Sigg, Stefan W Ballmer, Lisa Barsotti, Nergis Mavalvala, and Matthew Evans. Gravitational wave detector with cosmological reach. *Physical Review D*, 91(8):082001, 2015.
- [54] Matthew Abernathy, F Acernese, P Ajith, B Allen, P Amaro-Seoane, et al. Einstein gravitational wave telescope conceptual design study. *available from European Gravitational Observatory, document number ET-0106A-10*, 2011.
- [55] P. Christian, S. Vitale, and A. Loeb. in prep.